CHEMISTRY
A European Journal

A Journal of
ChemPubSoc Europe

Accepted Article

Title: Complexation and Versatile Reactivity of a Highly Lewis Acidic Cationic Mg Complex with Alkynes and Phosphines

Authors: Jürgen Pahl, Tom E. Stennett, Michel Volland, Dirk Guldi, and Sjoerd Harder

To be cited as: *Chem. Eur. J.* 10.1002/chem.201804802

Link to VoR: http://dx.doi.org/10.1002/chem.201804802

Supported by
ACES

WILEY-VCH

10.1002/chem.201804802

Complexation and Versatile Reactivity of a Highly Lewis Acidic Cationic Mg Complex with Alkynes and Phosphines

Jürgen Pahl[a], Tom E. Stennett[a], Michel Volland[b], Dirk Guldi[b], Sjoerd Harder*[a]

[a] *Inorganic and Organometallic Chemistry, Friedrich-Alexander-Universität Erlangen-Nürnberg, Egerlandstraße 1, 91058 Erlangen, Germany.*

[b] Lehrstuhl für Physikalische Chemie I, *Friedrich-Alexander-Universität Erlangen-Nürnberg, Egerlandstraße 3, 91058 Erlangen, Germany.*

Figure Table of Contents

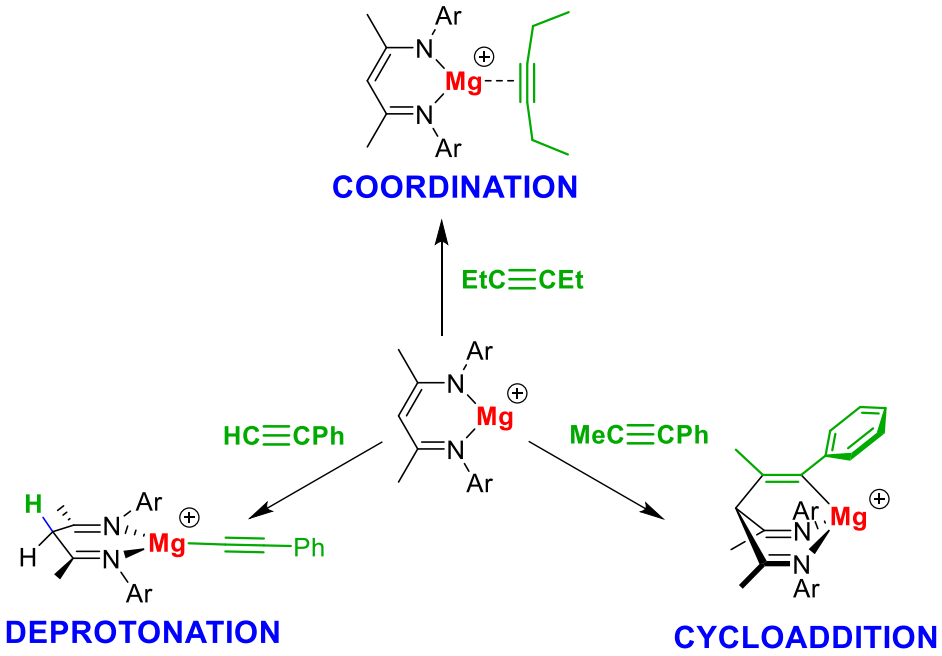

Keywords Magnesium – Cations – Lewis acidity – Frustrated Lewis Pair

Abstract

[(BDI)Mg^+][$B(C_6F_5)_4^-$] **1** (BDI = $CH[C(CH_3)N\text{-}Dipp]_2$; Dipp = 2,6-diisopropylphenyl) was prepared by reaction of (BDI)Mg*n*Pr with [Ph_3C^+][$B(C_6F_5)_4^-$]. Addition of 3-hexyne gave [(BDI)Mg^+·(EtC≡CEt)][$B(C_6F_5)_4^-$]. Single crystal X-ray analysis, NMR investigations, Raman spectra and DFT calculations indicate a significant Mg-alkyne interaction. Addition of the terminal alkynes for PhC≡CH or Me_3SiC≡CH led to alkyne deprotonation by the BDI ligand to give [(BDI-H)Mg^+(C≡CPh)]$_2$ 2[$B(C_6F_5)_4^-$] (**2**, 70%) and [(BDI–H)Mg^+(C≡CSi$(CH_3)_3$)]$_2$ 2[$B(C_6F_5)_4^-$]

(**3**, 63%). Addition of internal alkynes PhC≡CPh or PhC≡CMe led to a [4+2]-cycloaddition with the BDI ligand to give $\{Mg^+C(Ph)=C(Ph)C[C(Me)=NDipp]_2\}_2$ $2[B(C_6F_5)_4^-]$ **4** (53%) and $\{Mg^+C(Ph)=C(Me)C[C(Me)=NDipp]_2\}_2$ $2[B(C_6F_5)_4^-]$ **5** (73%) in which the Mg metal is (*N*,*N*,*C*)-chelated. The $(BDI)Mg^+$ cation can be seen as an intramolecular Frustrated Lewis Pair (FLP) with a Lewis acidic site (Mg) and a Lewis (or Brønsted) basic site (BDI). Reaction of $[(BDI)Mg^+][B(C_6F_5)_4^-]$ **1** with a range of phosphines varying in bulk and donor strength led to formation of $[(BDI)Mg^+{\cdot}PPh_3][B(C_6F_5)_4^-]$ (**6**), $[(BDI)Mg^+{\cdot}PCy_3][B(C_6F_5)_4^-]$ (**7**) and $[(BDI)Mg^+{\cdot}P\textit{t}Bu_3][B(C_6F_5)_4^-]$ (**8**). The bulkier phosphine $PMes_3$ did not show any interaction. Combinations of $[(BDI)Mg^+][B(C_6F_5)_4^-]$ and phosphines did not result in addition to the triple bond in 3–hexyne but during the screening process it was discovered that the cationic magnesium complex catalyses the hydrophosphination of PhC≡Ch with $HPPh_2$ for which tentatively an FLP-type mechanism is proposed.

Introduction

Activation of molecules by interaction with a strong Lewis acid is one of the most fundamental principles in organic chemistry and has also has been exploited in catalysis.[1] Whereas most Lewis acids are based on *p*-block elements (notably B and Al), we recently introduced a set of highly Lewis acidic cationic alkaline earth metal complexes that are stabilized by the (*N*,*N*)-chelating ß-diketiminate ligand BDI (BDI = $CH[C(CH_3)N\text{-}Dipp]_2$; Dipp = 2,6-diisopropylphenyl). In contrast to earlier reported cationic BDI alkaline earth metal complexes,[2] these cations are free of Lewis bases and consequently are able to form strong adducts with benzene (**I**) or with 3-hexyne (**II**).[3] Competition experiments showed that $(BDI)Mg^+$ is even more Lewis acidic than the corresponding Al cation, $(BDI)AlMe^+$, or the benchmark Lewis acid $B(C_6F_5)_3$. Notably, the cation $(BDI)Mg^+$ is able to bind the otherwise fully inert silyl ether $O(SiMe_3)_2$ (**III**).[4] The high Lewis acidity of these cations may be exploited in molecule activation and could have applications in the rapidly growing field of Frustrated Lewis Pair (FLP) chemistry. Indeed, a combination of Lewis acidic $(BDI)Ca^+$ and Lewis basic $(BDI)Al^I$ strikingly dearomatize C_6H_6 to give formally a $C_6H_6^{2-}$ species (**IV**).[5]

Herein we report on extensive investigations of $(BDI)Mg^+$-alkyne reactivity which depending on the alkyne can follow the pathways of (i) coordination, (ii) deprotonation or (iii) cycloaddition. Since $(BDI)Mg^+$ may have potential as a strong Lewis acid in FLP chemistry, the

10.1002/chem.201804802

interaction with a variety of phosphines is studied in detail. Since there are only very few examples of Mg/P FLPs,[6] we also explore the possibility of alkyne activation by (BDI)Mg^+/phosphine combinations.

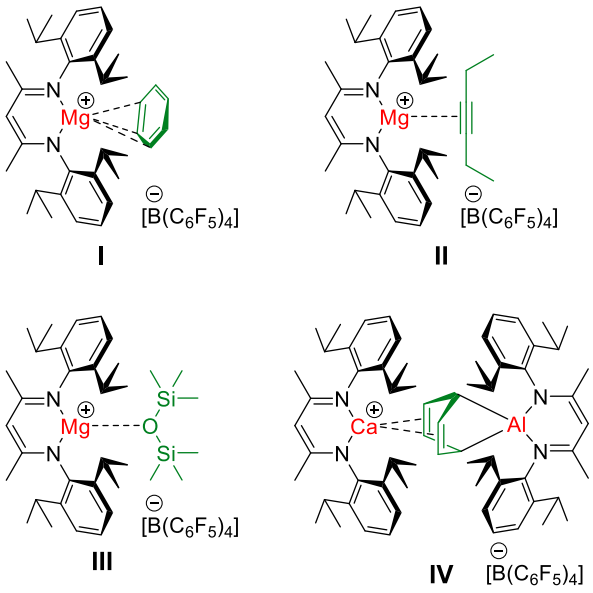

Results and Discussion

Mg-Alkyne coordination

Our previously reported magnesium alkyne complex [(BDI)Mg^+·EtC≡CEt][$B(C_6F_5)_4^-$] (**II**) was prepared by generating the (BDI)Mg^+ cation followed by addition of 3-hexyne (Scheme 1). Its crystal structure (Figure 1) shows slightly asymmetric Mg-alkyne bonding (Mg-C: 2.399(2)/2.480(2) Å; Mg-CC_{center}: 2.360(1) Å) complemented by bidentate coordination of the BDI ligand as well as a Mg···F contact to the weakly coordinating anion $B(C_6F_5)_4^-$. Agostic CH_2···Dipp π–interactions (Figure 1b) lead to additional stabilization of this Mg-alkyne complex.

The bonding situation in **II** can best be understood by a comparison with other 3-hexyne coordination complexes, e.g. with the coinage metal complexes (Cu, Ag, Au), bearing a sterically very similar β–diketiminate ligand $[N\{C(C_3F_7)N(Dipp)\}_2]^-$,[7] or with the Fe(I) complex (BDI)Fe·EtC≡CEt.[8] The most important geometric features are summarized in Table 1. The C≡C bond in the Mg-alkyne complex **II** is, at 1.193(3) Å, only marginally elongated compared to a typical unactivated (C,H)C≡C(C,H) bond (1.181 Å).[9] In comparison, coinage metal-alkyne

10.1002/chem.201804802

complexes show slightly longer C≡C bonds (1.216(3)-1.233(7) Å). Not surprisingly, the longest C≡C bond (1.263(4) Å) is found in the Fe-alkyne complex in which partially filled *d*-orbitals effectively activate the triple bond by strong π-backdonation. Although the triple bond in the Mg-alkyne complex is barely elongated, it is partially activated for nucleophilic attack through polarization of the π-electron density. This is illustrated by a significant deviation of the alkyne ligand from linearity: the C≡C–C angles in **II** vary from 170.7(2)° to 172.0(2)°. Distortion from linearity increases with increasing C≡C bond lengths and is most pronounced for the Fe-alkyne complex in which C≡C–C angles down to 148.5(3)° have been measured.

Table 1. Comparison of metal-(3-hexyne) complexes with free 3-hexyne; distances in Å and angles in degrees.

	3-hexyne	Mg[3]	Ag[7]	Cu[7]	Au[7]	Fe[8]
C≡C (Å)	1.181[a]	1.193(3)	1.216(3)	1.233(3)	1.233(7)	1.263(4)
C≡C–C (°)	180[b] 180	170.7(2) 172.0(2)	164.7(2) 165.3(2)	156.3(2) 156.5(2)	155.0 155.7	148.5(3) 148.9(3)
Raman (cm^{-1})	2228 2244 2296	2193 2240	2104	2003	1920	- - -
IR (cm^{-1})	2120	-	-	-	-	1802

[a] Average value for a (C,H)C≡C(C,H) bond.[9] [b] Idealized value.

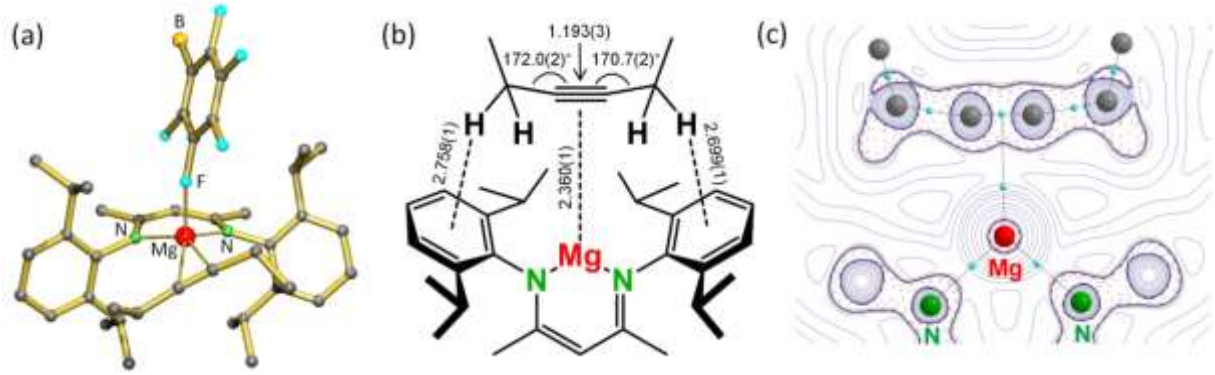

Figure 1. (a) Crystal structure of $[(BDI)Mg^{+}\cdot EtC{\equiv}CEt][B(C_6F_5)_4^{-}]$ (H atoms not shown, anion only partially shown). Selected bond distances (Å) and angles (°): Mg–N1 1.978(1), Mg–N2 1.994(1), Mg–F1 2.066(1), Mg–C32 2.480(2), Mg–C33 2.399(2). (b) Characteristic bond lengths (Å) and angles (°) in $[(BDI)Mg^{+}\cdot EtC{\equiv}CEt][B(C_6F_5)_4^{-}]$. (c) QTAIM representation of the Laplacian of the electron density in **II** in the plane through Mg and C≡C (bond critical points are indicated by light-blue spheres).

As in the case of the coinage metal-alkyne complexes, attempts to obtain additional information about the 3–hexyne activation by IR spectroscopy were unsuccessful (Supporting Information). Whereas the C≡C vibrations in (BDI)Mg^+·EtC≡CEt could not unequivocally be detected in the IR spectrum, the Raman spectroscopy gave signals at 2193 and 2240 cm^{-1}, corresponding to the C≡C unit. The calculated C≡C frequency of 3-hexyne (2287 cm^{-1}) is significantly higher than values observed for **II**. A direct comparison with free 3-hexyne is difficult due to the Fermi coupling in this region (bands at 2228 cm^{-1}, 2244 cm^{-1}, and 2296 cm^{-1}).[10] It is, however, clear that the C≡C frequencies for the coinage metal-(3-hexyne) complexes are substantially smaller than those for **II**. The lowest frequency is found for the Fe-(3-hexyne) complex for which only an IR vibration has been reported.

Previous DFT calculations (ωB97X/6-311+G**) have shown that the Mg-alkyne interaction in **II** is largely electrostatic: the total NPA charge of +0.042 on 3-hexyne suggests negligible alkyne → Mg electron transfer.[3] Complexation of 3-hexyne by the "naked" (BDI)Mg^+ cation results in a total energy gain of ΔE = -43.1 kcal mol^{-1} and is therefore more exothermic than benzene coordination: ΔE = -36.1 kcal mol^{-1}. This may partially originate from agostic CH_2···Dipp π–interactions which, like in the crystal structure, are also observed in the calculated structure. QTAIM analysis of the electron density in **II** clearly shows a strong polarization of the tubular C≡C π-electron density. This is not only evident from the ellipticity parameter of 0.0822 a.u. which deviates from zero, the expected value for a cylindrical electron distribution, but most clearly illustrated by the Laplacian of the electron density (Fig. 1c). This visualization shows a bond path from Mg to the middle of the C≡C bond and a strong polarization of the C≡C electron density towards the metal.

The Mg-alkyne complex **II** does not dissolve in benzene or toluene and loses its alkyne ligand in polar solvents like THF. Dissolved in a polar non-coordinating solvent like chlorobenzene, however, the Mg-alkyne bond remains intact. This is clear from a considerable upfield shift of the ^1H NMR signals for coordinated 3-hexyne. Especially the CH_2 group signal, which shifts from 2.07 ppm (free 3-hexyne) to 1.42 ppm, is indicative of strong bonding. This upfield shift may be due the CH_2···Dipp π–interactions, originating from ring current effects in the Dipp substituents. Similar upfield shifts have been recorded for the previously discussed coinage metal complexes.[7] The preference of (BDI)Mg^+ to coordinate 3-hexyne *versus* benzene (DFT: ΔE = 7.0 kcal/mol) can also be confirmed in solution by a competition experiment. Addition of two equivalents of benzene to **II** dissolved in C_6D_5Br gave no changes in the ^1H

NMR chemical shifts (Supporting Information). Significant broadening of the CH_2 signals, however, indicate an equilibrium between alkyne *versus* benzene coordination which is largely at the alkyne side. The quaternary carbon atom of the C≡C unit could not be detected by ^{13}C NMR spectroscopy, precluding further conclusions on the bonding situation.

Alkyne reactivity

In order to increase our understanding of Mg-alkyne complexes we explored complexation with terminal alkynes or internal alkynes containing Ph substituents. The latter group of ligands may provide information on the preference for Ph *versus* alkyne bonding. In all cases, however, we observed a distinct alkyne transformation instead of simple coordination.

Reaction of the *in–situ* generated "naked" cationic complex **1** with the terminal alkynes PhC≡CH and $Me_3SiC{\equiv}CH$ led to alkyne deprotonation by the BDI ligand (Scheme 1). In a similar fashion to the previously reported reaction of **1** with water,[11] the anionic BDI ligand is converted to a neutral *bis*-imine ligand and the Mg-alkynide complexes $[(BDI\text{-}H)Mg^{+}CCPh]_2{\cdot}2[B(C_6F_5)_4^{-}]$ (**2**) and $[(BDI\text{-}H)Mg^{+}CCSi(CH_3)_3]_2{\cdot}2[B(C_6F_5)_4^{-}]$ (**3**) were isolated in yields of 70% and 63%, respectively. This cooperative acid-base transformation may be described as intramolecular Frustrated Lewis Pair (FLP) reactivity and is analogous to (alkyne)C-H bond cleavage by the FLP $Cp_2Zr(OAr)^{+}/PCy_3$.[12] Interestingly, the reaction with PhC≡CH to form complex **2** takes less than 5 minutes at room temperature whereas deprotonation of this alkyne by $(BDI)MgN(SiMe_3)_2$ to give (BDI)MgC≡CPh needs forcing conditions (60°C, 60 h).[13] Given the pK_a value of 22.6 for PhC≡CH,[14] deprotonation of the alkyne by an otherwise innocent BDI ligand is unusual. The analogous conversion of $Me_3SiC{\equiv}CH$ to form complex **3** needs much more forcing conditions (80°C, 1 h). Since the pK_a values of both alkynes are expected to be similar, the nature of the Ph group seems to be essential for fast conversion. We propose a mechanism in which the Ph group coordinates to the Lewis acidic Mg center. This leads to strong charge polarization and acidification of the alkyne C-H group which subsequently is easily deprotonated by the BDI backbone. The synthesis of complexes **2** and **3** can also be accomplished by starting from the arene adduct $[(BDI)Mg^{+}{\cdot}C_6H_6]$ $[B(C_6F_5)_4^{-}]$ indicating that terminal alkynes may compete with benzene for Mg coordination.

10.1002/chem.201804802

Since the BDI ligand in (BDI)Mg^+ is too Brønsted basic to tolerate terminal alkynes with pK_a values around 23 (pK_a PhC≡CH: 22.6),[14] we focussed on coordination of internal alkynes. Layering an *in situ* generated solution of [(BDI)Mg^+][$B(C_6F_5)_4^-$] in chlorobenzene with a hexane solution of PhC≡CPh or PhC≡CMe led to crystallization of the products **4** and **5** in yields of 53% and 75%, respectively (Scheme 1). This [4+2]-cycloaddition does not proceed in the presence of benzene; in this case the benzene adduct (BDI)$Mg^+ \cdot C_6H_6$ is formed. This indicates that benzene coordinates more strongly than Ph-substituted internal alkynes. It is likely that the observed cycloaddition proceeds by Mg-alkyne coordination followed by intramolecular nucleophilic attack by the BDI ligand. Since the alkyne EtC≡CEt does not show cycloaddition, alkyne activation through Ph-Mg coordination and triple bond conjugation with at least one Ph group is crucial. The herein observed [4+2]-cycloaddition is limited to a few metal complexes of which all except one feature cationic metal centers (Pt, Al^+, Ru^+, Os^+).[15] It is of interest to note that reaction of (BDI)Mg^+ with the unsymmetrical internal alkyne PhC≡CMe selectively gives BDI attack at the Me-substituted carbon atom. This contrasts with the reactivity of (BDI)$AlMe^+$ with PhC≡CH in which attack occurs selectively at the Ph-substituted carbon atom.[8] Electronic arguments (+I effect of Me) and steric arguments (small Me substituent facing the bulky Dipp ligands) are in favour of the latter. The unusual selectivity observed in (BDI)Mg^+/PhC≡CMe cycloaddition may be explained by initial coordination of the substrate via its aromatic ring. This leads to polarization of the C≡C bond facilitating BDI attack at the Me-substituted carbon atom.[16]

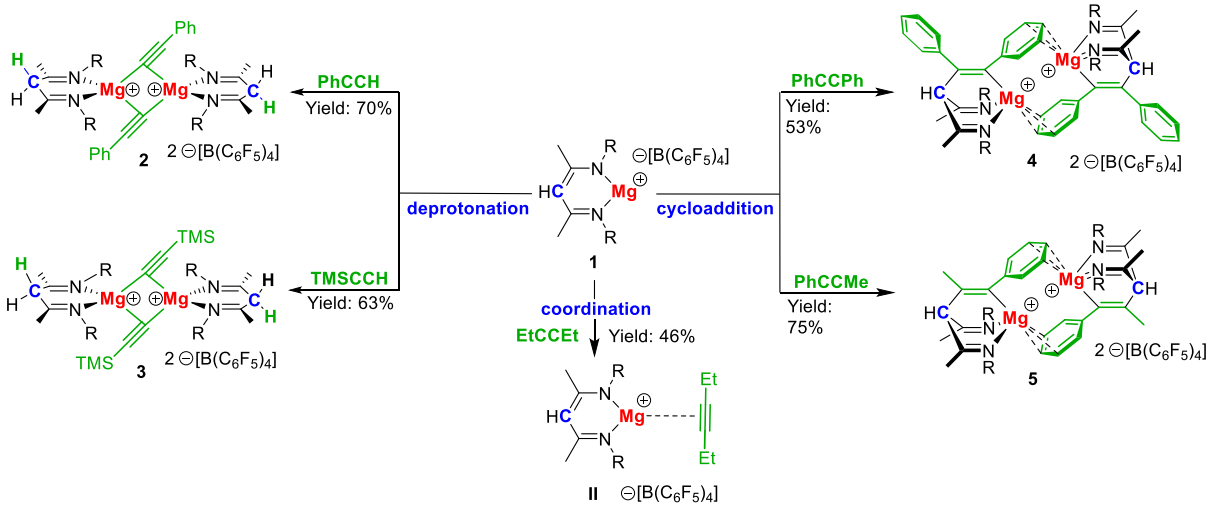

Scheme 1. Reactivity of [(BDI)Mg^+][$B(C_6F_5)_4^-$] with alkynes (R = Dipp).

10.1002/chem.201804802

*Crystal structures and solution investigations of complexes **2** and **3***

Crystal structures of complexes **2** and **3** are displayed in Figure 2. Similarly as for $[(BDI)Mg(C{\equiv}CPh)]_2$,[13] the complexes are dimeric featuring an asymmetric bridging alkynide. The latter shows a combination of Mg-C σ-bonding (along the *sp*-hybrid orbital) and side-on π-interaction. Whereas the Mg-C σ-bonds (Mg–C30; **2:** 2.154(3) Å; **3:** 2.170(2) Å) compare well to that in $[(BDI)Mg(C{\equiv}CPh)]_2$ (2.174(2) Å), the side-on π-bonds are clearly more asymmetric than in the neutral dimer (**2:** 2.250(3)/2.868(3), **3:** 2.268(2)/2.751(2) Å, $[(BDI)Mg(C{\equiv}CPh)]_2$: 2.349(2)/2.671(2) Å). This may be explained by the steric repulsion between the CH_2 group of the neutral BDI ligand, which is in a boat conformation, and the alkyne. Protonation of the BDI anion is confirmed by typical C=N bond distances (**2**: C=N 1.285 Å, **3**: C=N 1.284 Å) as well as by the C-C distances (**2**: 1.518 Å, **3**: 1.517 Å). Description of the BDI ligand as a diimine is supported by IR spectra in which clear signals for a C=N vibration can be observed (**2**: 1617 cm^{-1}, **3**: 1620 cm^{-1}). Although for **3** no absorption associated with a C≡C stretch vibration could be observed, the C≡C vibrational frequency of complex **2** could be detected at a wavenumber of 2050 cm^{-1}. This compares well with that in $[(BDI)Mg(C{\equiv}CPh)]_2$ observed at 2047 cm^{-1}.

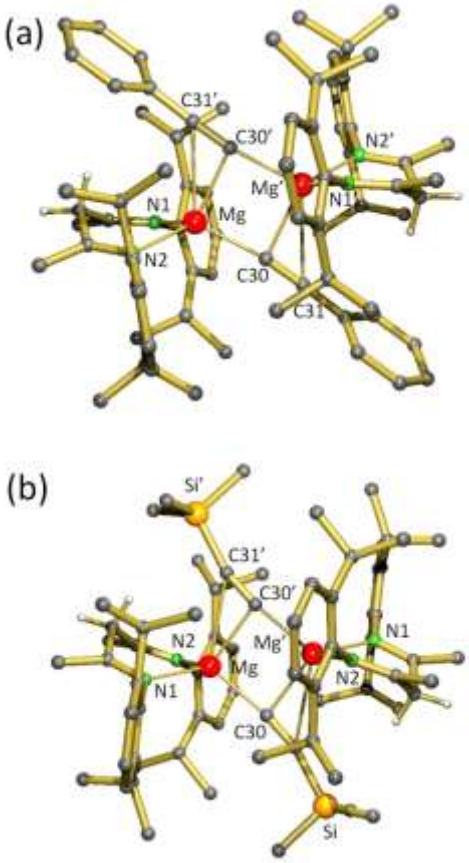

Figure 1. (a) Crystal structure of $[(BDI\text{-}H)Mg^{+}CCPh]_2{\cdot}2[B(C_6F_5)_4^{-}]$ (**2**) (H atoms and anion not shown). Selected bond distances (Å) and angles (°) in one of the independent dimers: Mg–N1 2.106(3), Mg–N2 2.121(3), Mg–C30 2.154(3), Mg–C30' 2.250(3), Mg–C31' 2.868(3), C2–N1 1.285(4), C4–N2 1.284(4), N2–Mg–N1 92.12(10). (b) Crystal structure of $[(BDI\text{-}H)Mg^{+}CCSiMe_3]_2{\cdot}2[B(C_6F_5)_4^{-}]$ (**3)** (H atoms and anion not shown). Selected bond distances (Å) and angles (°): Mg–N1 2.124(1), Mg–N2 2.131(2), Mg–C30 2.170(2), Mg–C30' 2.268(2), Mg–C31' 2.751(2), C2–N1 1.281(2), C4–N2 1.286(2) N2–Mg–N1 92.17(6).

NMR investigations on the dimeric complexes **2** and **3** were hampered by their very poor solubility in chlorobenzene which likely originates from their dicationic nature. Screening various solvent mixtures, we found that small amounts of complex **3** dissolve in 1,2-difluorobenzene/C_6D_6 (2/1). The ^1H NMR spectrum of **3** in this solvent mixture features two doublets at

10.1002/chem.201804802

3.79 and 3.92 ppm ($^2J_{HH}$ = 17.5 Hz) for the diastereotopic protons of the BDI-CH_2 group, indicating that asymmetric alkynide bridging is retained in solution. The ^{13}C NMR spectrum shows a resonance at 45.8 ppm for the BDI-CH_2 group, which is circa 45 ppm upfield with respect to the backbone CH signal in anionic BDI ligands. Both carbon atoms of the C≡C bond can be observed in the ^{13}C NMR spectrum at 100.3 and 115.0 ppm which is the expected region for Mg alkynide complexes. The signals are slightly upfield from values reported for $[(BDI)Mg(C{\equiv}CPh)]_2$ (111.2 and 122.0 ppm).[13]

Complex **2** is, once crystallized, completely insoluble. However, *in situ* generation of this complex in 1,2-difluorobenzene/C_6D_6 allowed for a circa ten hour time slot to study this complex in solution (longer measurement times are plagued by product crystallization). The NMR data for **2** are essentially the same as for complex **3** (see Experimental Section).

*Crystal structures and solution investigations of complexes **4** and **5***

The crystal structures of complexes **4** and **5** are depicted in Figure 3. The [4+2]-cycloaddition of the alkyne to $(BDI)Mg^+$ created a (*N*,*N*,*C*)-chelating tridentate ligand for Mg. In contrast to $(BDI)Mg^+$, which in exclusion of aromatic solvents shows strong interactions with the $B(C_6F_5)_4^-$ anion, the Mg centers in **4** and **5** prefer to interact with the Ph ring of a neighbouring cation: the shortest Mg···C contacts measure 2.360(2) Å (**4**) and 2.341(3) Å (**5**). This may be explained by the higher denticity of the tricoordinate ligand, leaving less space for cation···anion interaction, but could also originate from charge delocalization of formally negatively charged carbon C30 into the Ph ring. This would explain exclusive bridging of cations by the Ph substituent instead of by Dipp-substituents. The Mg-C bond lengths in **4** (2.122(2) Å) and **5** (2.100(3) Å) lie in the expected range.[9] The C30-C31 bond distances are in the characteristic range for a double bond (**4**: 1.344(3) Å, **5**: 1.336(4) Å). In contrast, the newly formed bond between the BDI ligand and the alkyne (C3-C31) is in both complexes significantly longer than an average (sp^3)C–C(sp^2) bond of 1.507 Å[9] (**4**: 1.574(2) Å, **5**: 1.566(4) Å). Such elongation is typical for these kind of complexes[15] and is in agreement with the reversibility of the cycloaddition reaction.

10.1002/chem.201804802

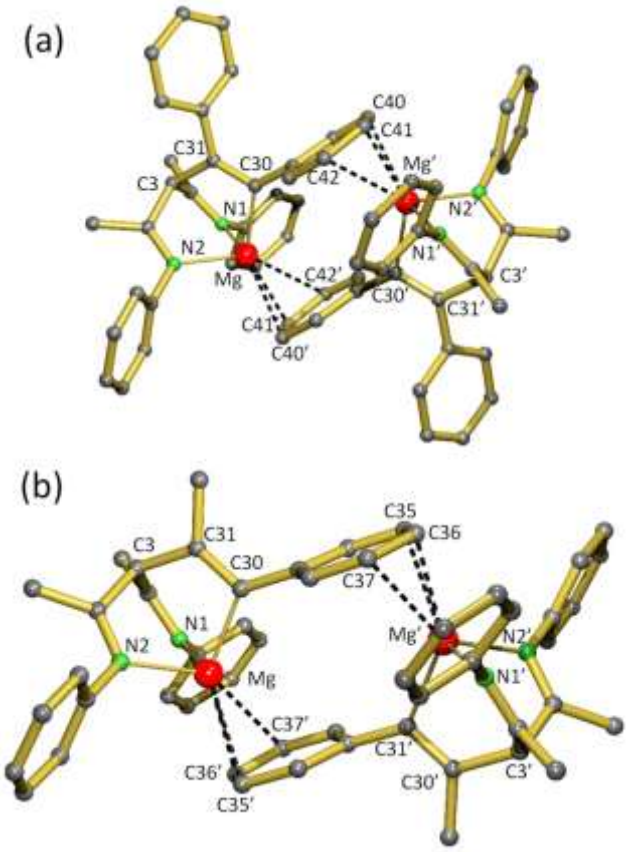

Figure 2. (a) Crystal structure of $\{Mg^{+}C(Ph)=C(Ph)C[C(Me)=NDipp]_2\}_2\cdot 2[B(C_6F_5)_4^{-}]$ (**4**) (H atoms, *i*Pr–groups and anion not shown). Selected bond distances (Å) and angles (°): Mg–N1 2.1382(16), Mg–N2 2.1411(16), Mg–C30 2.1218(18), Mg–C41' 2.3604(19), C2–C31 1.574(2), C30–C31 1.344(3) N2–Mg–N1 93.22(6). (b) Crystal structure of $Mg^{+}C(Ph)=C(Me)C[C(Me)=NDipp]_2\}_2\cdot 2[B(C_6F_5)_4^{-}]$ (**5)** (H atoms, *i*Pr–groups and anion not shown). Selected bond distances (Å) and angles (°) in one of the independent dimers: Mg–N1 2.148(2), Mg–N2 2.131(2), Mg–C30 2.100(3), Mg–C36' 2.341(3), C2–C31 1.566(4), C30–C31 1.336(4) N2–Mg–N1 93.21(9).

IR spectra of **4** and **5** were recorded in the solid state. Both complexes show absorbance at 1614 cm^{-1}, conclusive for formation of a C=N bond. The signals for the C=C double bonds lie in the same region (**4**: 1578 cm^{-1}, **5**: 1583 cm^{-1}).

NMR studies on complex **4** were precluded by the complete insolubility of this dicationic dimer in halogenated arenes. Addition of C_6D_6 as a weakly π-coordinating solvent to break the dimer into benzene ligated monomers resulted in the elimination of PhC≡CPh and the formation of $(BDI)Mg^{+}\cdot C_6D_6$. This is consistent with the observation that complex **4** cannot be synthesized in the presence of benzene. The reversibity of the [4+2]-cycloaddition was also observed in weakly coordinating solvents like fluorobenzene and 1,2-difluorobenzene.

Complex **5** could be dissolved in a mixture of C_6D_6 and C_6D_5Br at room temperature but heating this solution to 60 °C led to PhC≡CMe elimination and formation of $(BDI)Mg^{+}\cdot C_6D_6$.

NMR data at room temperature corroborate the previously presented characterization by X-ray diffraction and IR spectroscopy. The ^{1}H NMR signal for the proton attached to the now sp^{3} hybridized backbone carbon atom is strongly shifted upfield to 4.39 ppm. Moreover, the quaternary carbon atoms of the C=N moiety (182.5 ppm) as well as the C=C unit (175.1 ppm and 139.5 ppm) could be identified and unambiguously assigned by ^{1}H,^{13}C-correlated NMR measurements (Supporting information).

Mg-phosphine coordination

Evidence for unsupported interactions of magnesium complexes with neutral phosphine ligands are limited to the small phosphine PMe_3 or *P*,*P*-chelating ligands.[17] The recent isolation of $[(BDI)Mg^{+}\cdot PPh_3][Al(OC(CF_3)_3)_4^{-}]$[17c] illustrates that there is ample space at the metal atom in $(BDI)Mg^{+}$ to complex a larger phosphine. Herein we investigate the interaction of $(BDI)Mg^{+}$ with a series of phosphines of increasing bulk and/or donor properties. In order to assess the spatial accessibility of the metal atom in $(BDI)Mg^{+}$, coordination of triaryl- or trialkyl-phosphines with increasing Tolman angles was attempted: PPh_3 (145°) < PCy_3 (170°) < P*t*Bu_3 (182°) < $PMes_3$ (212°).[18] Donor strength is increased by replacing aryl substituents with alkyl groups. Adduct formation was investigated by addition of these phosphines to a solution of $[(BDI)Mg^{+}\cdot C_6D_6][B(C_6F_5)_4^{-}]$ in C_6D_5Br and measurement of ^{1}H, ^{13}C and ^{31}P NMR spectra.

Addition of one equivalent of PPh_3 led to a complex with ^{1}H and ^{13}C NMR chemical shifts that, despite use of a different solvent, closely match those for $[(BDI)Mg^{+}\cdot PPh_3][Al(OC(CF_3)_3)_4^{-}]$.[17c] The ^{31}P signal at -5.0 ppm is basically identical to that reported by Hill and coworkers (-4.9 ppm). Using the sterically more demanding PCy_3 also gave an adduct, indicated by a large downfield shift of the ^{31}P NMR signal for free PCy_3 (9.6 ppm) to 20.4 ppm. However, addition of P*t*Bu_3 led to slow conversion of the Lewis base into unidentified species. This is presumably due to reaction with the solvent. Change of the solvent for a mixture C_6H_5F/C_6D_6 or C_6H_5Cl/C_6D_6 prevented decomposition and led to a double set of BDI signals that likely originate from $(BDI)Mg^{+}\cdot P$*t*Bu_3 and $(BDI)Mg^{+}\cdot C_6D_6$ (50:50 ratio in C_6H_5F/C_6D_6 and 80:20 ratio in C_6H_5Cl/C_6D_6) suggesting that the formation of the Mg-P*t*Bu_3 adduct is a solvent-dependent equilibrium. This equilibrium is supported by the ^{31}P NMR spectrum, which shows two singlets, one of which one can be assigned to free P*t*Bu_3

10.1002/chem.201804802

(62.1 ppm). The other is shifted downfield (69.7 ppm), typical for (BDI)Mg^+-phosphine coordination. By far the bulkiest phosphine, $PMes_3$, did not show any sign of interaction with (BDI)Mg^+ in C_6D_5Br solution.

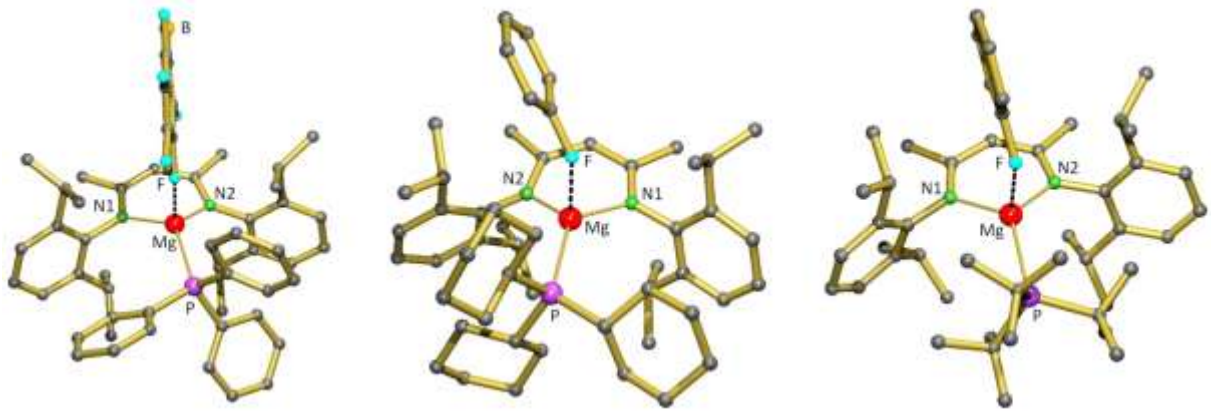

Figure 4. Crystal structures of [(BDI)Mg^+·PPh_3][$B(C_6F_5)_4^-$] **6**, [(BDI)Mg^+·(PCy_3)(PhF)][$B(C_6F_5)_4^-$] **7** and [(BDI)Mg^+·(P^tBu_3)(PhF)][$B(C_6F_5)_4^-$] **8**. Distances and angles can be found in Table 2.

Table 2. Selected bond distances (Å) and angles (°) for complexes **6**, **7**, **8** in comparison with those in [(BDI)Mg^+·PPh_3][$Al(OC(CH_3)_3)_4$].[17c]

Complex	[(BDI)Mg^+·PPh_3] [$Al(OC(CH_3)_3)_4^-$]	[(BDI)Mg^+·PPh_3] [$B(C_6F_5)_4^-$] **6**	[(BDI)Mg^+·PCy_3] [$B(C_6F_5)_4^-$] **7**	[(BDI)Mg^+·P^tBu_3] [$B(C_6F_5)_4^-$] **8**
Mg···P	2.597(1)	2.6549(5)	2.6551(6)	2.772(1)
C–N–C	120.9(3) 118.9(3)	117.6(1) 117.3(1)	118.5(1) 120.3(1)	119.0(2) 116.3(2)
Mg···F	-	2.1705(8)	2.1300(9)	2.075(2)
Mg–N	1.977(3) 1.983(3)	2.005(1) 2.013(1)	2.021(1) 2.029(1)	2.044(2) 2.060(2)

Isolation of well-defined (BDI)Mg^+-phosphine adducts turned out to be troublesome due to difficulties in the crystallization of their $B(C_6F_5)_4^-$ salts. Only the PCy_3 adduct could be isolated in a very low yield of 5% and was fully characterized. From the other adducts we have managed to isolate a few crystals that allowed for determination of their crystal structures, giving insights into structural changes upon variation of phosphine bulk and donor properties. Figure 4 shows the crystal structures of [(BDI)Mg^+·PPh_3][$B(C_6F_5)_4^-$] (**6**), [(BDI)Mg^+·(PCy_3)(PhF)][$B(C_6F_5)_4^-$] (**7**) and [(BDI)Mg^+·(P^tBu_3)(PhF)][$B(C_6F_5)_4^-$] (**8**); selected geometric parameters are summarized in Table 2. Whereas the previously reported [(BDI)Mg^+·PPh_3][$Al(OC(CF_3)_3)_4^-$] is a truly separated ion pair,[17c] the crystal structure of

[(BDI)Mg^+·PPh_3][$B(C_6F_5)_4^-$] (**6**) shows a single Mg···F interaction. Consequently, the Mg-P bond in **6** (2.6549(5) Å) is slightly longer than that in its aluminate salt (2.597(1) Å).

The PCy_3 and P*t*Bu_3 adducts **7** and **8** crystallize similarly to **6**, but with an additional Mg···F contact, which in this case stems from cocrystallized fluorobenzene. All structures also display several C-H···C(π) bonding interactions between the phosphine and BDI ligands. Since the ligand arrangement and Mg coordination spheres in **6**-**8** are very similar, the influences of the phosphine ligand on the structure of the cation can be discussed. Changing the phosphine ligand from PPh_3 to PCy_3 gave an adduct with an equally long Mg-P bond length. Apparently, the expected elongation of the Mg-P distance by increasing the bulk is compensated by bond shortening due to the better donor abilities of PCy_3. The P*t*Bu_3 adduct **8** shows an exceptionally large Mg-P bond distance of 2.772(1) Å which is in line with the weaker Mg–P interaction already observed in solution. Complex **8** also features unusually long Mg-N bond distances. The bulky phosphine P*t*Bu_3 cannot fully enter the free coordination site at Mg and, being a strong Lewis base, pulls the Mg metal away from the BDI ligand. The combination of two large ligands, (BDI) and P*t*Bu_3, therefore results in inefficient ligand-Mg interaction and may explain why **8** feautures the shortest Mg···F distance.

Towards FLP reactivity

Having established the details of interaction of the "naked" $(BDI)Mg^+$ cation with a range of alkynes and phosphines, the question arose whether such highly Lewis acidic cations may be used as components in Frustrated Lewis Pairs. Investigation of five different alkynes led to the conclusion that only *bis*-alkyl substituted alkynes, *e.g.* EtC≡CEt, do not react with the Lewis acid alone. Investigations of a range of phosphine complexes indicate that the larger weakly or non-bonding phosphines, P*t*Bu_3 and $PMes_3$, are likely the most successful Lewis bases for probing FLP reactivity. Our recent observation of alkyne addition to the adduct $(BDI)AlMe^+$·PPh_3,[8a] however, demonstrates that also adducts with smaller phosphines may be reactive. Thus, we investigated the FLP reactivity of EtC≡CEt in C_6D_5Br using [$(BDI)Mg^+$·C_6D_6][$B(C_6F_5)_4^-$] as the Lewis acid and the complete series of phosphines (PPh_3, PCy_3, P*t*Bu_3 and $PMes_3$) as the Lewis base. None of the phosphines displayed any reactivity towards the alkyne. Even the true FLP with the largest phosphine ligand, $(BDI)Mg^+$/$PMes_3$,

10.1002/chem.201804802

did not show any reaction with 3-hexyne, as apparent from ^{1}H NMR monitoring. Contrary to expectation, we made the observation that a very small phosphine, $HPPh_2$, in combination with $[(BDI)Mg^+\cdot C_6D_6][B(C_6F_5)_4^-]$ led to catalytic hydrophospination of PhC≡CH (Scheme 2; 10 mol% catalyst, 2:1 chlorobenzene/benzene, 60 °C, 20 hours, 72% conversion). Notably, a catalyst-free run under the same conditions gave no conversion. The reaction is slow but showed clean conversion to $H_2C{=}C(Ph)PPh_2$, the Markovnikoff product, and (*Z*)-$Ph(H)C{=}C(H)PPh_2$, the anti-Markovnikoff product in a ratio of 60/40. The exclusive formation of the *Z*-isomer of the anti-Markovnikoff product indicates that the H-PPh_2 to alkyne addition proceeds with a *trans*-selectivity. Although it was recently shown that hydrophosphination of PhC≡CH with $HPPh_2$ may proceed without solvent and catalyst (70 °C, 16 h, 80% conversion),[20] we could not reproduce these results. As we use very dry conditions and distilled substrates, small amounts of water may be necessary. Also the product distribution in the reported catalyst-free, thermally-induced, conversion is different (100% anti-Markovnikoff, *Z*/*E* = 95/5).[20]

The $(BDI)Mg^+$ catalyzed alkyne hydrophosphination reported here has a very limited scope. Internal alkynes did not react and also the terminal alkyne $Me_3SiC{\equiv}CH$ gave very poor conversion. Exchange of $HPPh_2$ for $HPCy_2$ gave under the same conditions only traces of the hydrophosphination product.

At this very preliminary stage we can only speculate about a possible mechanism. One could envision an FLP type mechanism in which the alkyne is activated for nucleophilic attack by Mg coordination. The current work shows that such Mg-alkyne complexes are feasible and that the alkyne is activated for nucleophilic attack by polarization of the π-electron density (Figure 1). In a subsequent step, the acidic phosphonium unit protonates the Mg-C bond, either directly or by H^+ transfer via the BDI backbone or $HPPh_2$. Examples of such H^+ transfer processes in FLP chemistry have been shown previously.[21] Although other mechanisms may be possible, this tentative FLP mechanism is formally a *trans*-addition of $HPPh_2$ to the alkyne, explaining the formation of an anti-Markovnikoff product exclusively as its *Z*-isomer. We are currently extending our explorations in this chemistry.

10.1002/chem.201804802

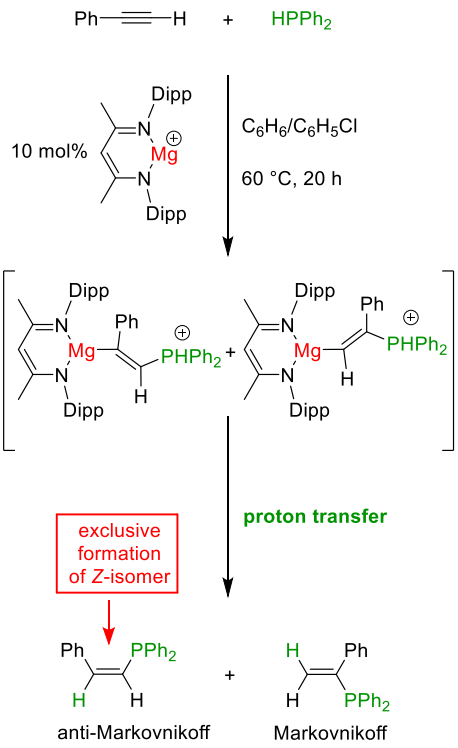

Scheme 2. Reaction of PhC≡CH with $HPPh_2$ catalyzed by $[(BDI)Mg^+{\cdot}C_6D_6][B(C_6F_5)_4^-]$. The exclusive formation of the *Z*-isomer for the anti-Markovnikoff product confirms rear-side attack of the alkyne by $HPPh_2$.

Conclusions

We have presented a detailed investigation of the interactions and reactivity of alkynes with the Lewis base-free, highly Lewis acidic, cationic magnesium complex $[(BDI)Mg^+{\cdot}C_6D_6][B(C_6F_5)_4^-]$. Alkyne-Mg bonding in the previously reported $[(BDI)Mg^+{\cdot}EtC{\equiv}CEt][B(C_6F_5)_4^-]$ is essentially electrostatic and results in negligible C≡C bond lengthening. A significant decrease in the Raman frequency for the C≡C vibration points to some bond weakening. As the C≡C electron density is strongly polarized towards the metal, the triple bond should be activated for rear-side nucleophilic attack. Use of terminal alkynes led to deprotonation of the alkyne by the BDI ligand. Internal alkynes containing at least one Ph group reacted by [4+2]-cycloaddition with the BDI ligand. In both transformations the $(BDI)Mg^+$ cation could be described as an internal FLP in which alkynes are activated by the combined interaction with Lewis acidic Mg and the Lewis basic BDI ligand. In addition, we have presented complexation of the $(BDI)Mg^+$ cation with a range of phosphines that vary in bulk and donor strength. Whereas there is evidence for complex formation with the phosphines PPh_3, PCy_3 and $PtBu_3$ in the solid state as well in solution, the largest phosphine

$PMes_3$ does not form a coordination complex on account of its extensive bulk. Although the latter Lewis acid-base combination $(BDI)Mg^+/PMes_3$ can be seen as a true FLP, no reaction with EtC≡CEt was observed. It was, however, observed that $(BDI)Mg^+$ is a catalyst for hydrophosphination of PhC≡CH with the secondary phosphine $HPPh_2$. Based on the exclusive formation of the *Z*-isomer for the *anti*-Markovnikoff product, tentatively a FLP-type mechanism is proposed: the alkyne is activated by formation of a Mg···alkyne complex and attacked from the rear by $HPPh_2$.

The results presented herein underscore the high Lewis acidity of Lewis base-free cationic Mg complexes. The results also show that the BDI ligand may not be the best platform for small molecule activation. Although the BDI ligand is generally a non-innocent spectator ligand, the high Lewis acidity of the Mg center activates alkynes to such an extent that the BDI ligand reacts either as a Brønsted base or as a nucleophile. We are currently working on as set of cationic Mg Lewis acids with more docile spectator ligands.

Experimental section

General Experimental Procedures

All experiments were conducted under an inert nitrogen atmosphere using standard Schlenk and glovebox techniques (MBraun, Labmaster SP). All solvents were degassed with nitrogen, dried over activated aluminium oxide (Solvent Purification System: Pure Solv 400−4−MD, Innovative Technology) and stored over 3Å molecular sieves. Fluorobenzene, chlorobenzene, bromobenzene, 1,2-difluorobenzene, phenylacetylene (Fluka, 97%), were dried over calcium hydride, distilled under N_2 atmosphere and stored over molecular sieves 3Å. Trimethylsilyacetylene (98%, Sigma Aldrich), Phenylpropyne (98%, abcr), 3–hexyne (99%, Sigma Aldrich) and diphenylphosphine (99%, abcr) were dried over molecular sieves 3Å. PPh_3 (99%, Alfa Aesar) was dried over P_2O_5 and recrystallized whereas $PtBu_3$ (99%, abcr) was used directly as received. C_6D_6 and C_6D_5Br (99.6% D, Sigma Aldrich) were dried over 3Å molecular sieves. $[Ph_3C^+][(C_6F_5)_4B^-]$ (Boulder Scientific) was used as received. $[(BDI)MgnPr]_2$,[3] $[(BDI)Mg^+{\cdot}EtC{\equiv}CEt][B(C_6F_5)_4^-]$,[3] $PMes_3$,[22] and $[(BDI)Mg^+{\cdot}C_6D_6][B(C_6F_5)_4^-]$[3] were synthesized according to literature procedures. NMR spectra were recorded with a Bruker Avance III HD 400 MHz or a Bruker Avance III HD 600 MHz spectrometer. The spectra were referenced to the respective residual signals of the deuterated solvents. Elemental analysis was performed

with a Euro EA 3000 (Euro Vector) analyzer or a Vario MICRO Cube (Elementar). IR spectra were measured on a ATR platinum T (Bruker) spectrometer. Raman measurements were carried out with a WITec alpha300 R using laser excitations of 532 nm. All crystal structures have been measured on a SuperNova (Agilent) diffractometer with dual Cu and Mo microfocus sources and an Atlas S2 detector. Crystallographic data have been deposited with the Cambridge Crystallographic Data Centre as supplementary publication no. 1867876 (**2**), 1867877 (**3**), 1867878 (**4**), 1867879 (**5**), 1867880 (**6**), 1867881 (**7**) and 1867882 (**8**). Copies of the data can be obtained free of charge on application to CCDC, 12 Union Road, Cambridge CB21EZ, UK (fax: (+44)1223-336-033; E-mail: deposit@ccdc.cam.ac.uk).

Synthesis of [(BDI-H)Mg$^+$(CCPh)]$_2$ 2[B(C$_6$F$_5$)$_4^-$] (2): [(BDI)Mg$^+$·C$_6$H$_6$][B(C$_6$F$_5$)$_4^-$] (0.051 g, 0.043 mmol) was dissolved in a mixture of 1,2-difluorobenzene (0.3 ml) and benzene (0.1 ml). After addition of phenylacetylene (6.0 µl, 0.055 mmol) the colorless solution was left standing for 1 day at room temperature for crystallization. The crystals were washed with chlorobenzene (2 x 0.1 ml). The product (**2**) was obtained as colorless crystals (0.037 g, 0.015 mmol) in a yield of 70%. Due to the insolubility of the product NMR data could only be obtained from an *in situ* prepared sample using C$_6$H$_4$F$_2$/C$_6$D$_6$ as a solvent. ^{1}H NMR (400 MHz, C$_6$H$_4$F$_2$/benzene-*d*$_6$, 298K) δ 3.45 (d, $^2J_{HH}$ = 16.4 Hz, 1H, CC*H*$_2$C), 3.08 (d, $^2J_{HH}$ = 16.4 Hz, 1H, CC*H*$_2$C), 2.48 (hept, $^3J_{HH}$ = 6.8 Hz, 2H, C*H*Me$_2$), 2.38 (hept, $^3J_{HH}$ = 6.8 Hz, 2H, C*H*Me$_2$), 1.60 (s, 6H, CC*H*$_3$), 1.19 (d, $^3J_{HH}$ = 6.8 Hz, 6H, CHC*H*$_3$), 0.97 (d, $^3J_{HH}$ = 6.8 Hz, 6H, CHC*H*$_3$), 0.90 (d, $^3J_{HH}$ = 6.8 Hz, 6H, CHC*H*$_3$), 0.38 (d, $^3J_{HH}$ = 6.8 Hz, 6H, CHC*H*$_3$), (all signals in the aromatic region are obscured by C$_6$H$_4$F$_2$); ^{13}C NMR (101 MHz, C$_6$H$_4$F$_2$/benzene-*d*$_6$, 298K) δ 186.3 (s, *C*=N), 139.5 (s, Ar*C*), 138.8 (s, Ar*C*), 132.2 (s, Ar*C*), 132.1 (s, Ar*C*), 129.5 (s, Ar*C*), 129.4 (s, Ar*C*), 125.7 (s, Ar*C*), 125.1 (s, Ar*C*), 118.3 (s, Mg*C*≡C) 104.2 (s, MgC≡*C*), 45.2 (s, C*C*H$_2$C), 30.1 (s, *C*HMe$_2$), 28.0 (s, *C*HMe$_2$), 26.2 (s, NC(*C*H$_3$)), 24.5 (s, CH*C*H$_3$), 23.8 (s, CH*C*H$_3$), 23.0 (s, CH*C*H$_3$), 22.5 (s, CH*C*H$_3$); ^{19}F NMR (376 MHz, C$_6$H$_4$F$_2$/benzene-*d*$_6$, 298K) δ -132.13 – (-132.47) (m, 8F, *o*-C*F*), -163.46 (t, $^3J_{FF}$ = 20 Hz, 4F, *p*-C*F*), -167.26 (t, *J* = 20 Hz, 8F, *m*-C*F*); ^{11}B NMR (128 MHz, C$_6$H$_4$F$_2$/benzene-*d*$_6$, 298K) δ -16.1 (s, *B*(C$_6$F$_5$)$_4$); IR (ATR, pure): ṽ = 2970 (m), 2931 (w), 2874 (w), 2050 (w), 1641 (m), 1617 (w), 1512 (s), 1460 (vs), 1371 (s), 1311 (s), 1266 (s), 1084 (vs), 977 (vs), 933 (m), 843 (m), 798 (s), 754 (vs), 682 (s), 660 (s); Elemental analysis calcd (%) for C$_{122}$H$_{94}$B$_2$F$_{40}$Mg$_2$N$_4$ (2446.29): C 59.90, H 3.87, N 2.29; found: C 59.72, H 3.74, N 1.72.

Synthesis of [(BDI-H)Mg$^+$(CCSi(CH$_3$)$_3$)]$_2$ 2[B(C$_6$F$_5$)$_4^-$] (3): [(BDI)Mg$^+$·C$_6$H$_6$][B(C$_6$F$_5$)$_4^-$] (0.101 g, 0.0842 mmol) and trimethylsilylacetylene (0.0120 ml, 0.0843 mmol) were dissolved in 1,2–difluorobenzene (1.0 ml) and heated to 80°C for 1 hour. The colorless solution was layered with hexane (0.3 ml) after which immediate crystallization was observed. Washing the crystals with fluorobenzene (5 x 0.3 ml) and subsequent drying *in vacuo* gave the desired product (**3**) in a yield of 63% (0.061 g, 0.025 mmol). Due to its extremely low solubility NMR data were recorded in a 2:1 mixture of $C_6H_4F_2$ and C_6D_6. ^{1}H NMR (600 MHz, $C_6H_4F_2$/benzene-d_6, 298K) δ 3.92 (d, $^2J_{HH}$ = 17.5 Hz, 2H, CC*H*$_2$C), 3.79 (d, $^2J_{HH}$ = 17.5 Hz, 2H, CC*H*$_2$C), 2.43 (hept, $^3J_{HH}$ = 6.9 Hz, 4H, C*H*Me$_2$), 2.20 (hept, $^3J_{HH}$ = 6.9, 4H, C*H*Me$_2$), 1.71 (s, 12H, CC*H*$_3$), 1.31 (d, $^3J_{HH}$ = 6.8 Hz, 12H, CHC*H*$_3$), 0.96 (d, $^3J_{HH}$ = 6.8 Hz, 12H, CHC*H*$_3$), 0.92 (d, $^3J_{HH}$ = 6.8 Hz, 12H, CHC*H*$_3$), 0.13 (d, $^3J_{HH}$ = 6.8 Hz, 12H, CHC*H*$_3$), 0.11 (s, 18H, Si*Me*$_3$), (all signals in the aromatic region were obscured by $C_6H_4F_2$); ^{13}C NMR (151 MHz, $C_6H_4F_2$/benzene-d_6, 298K) δ 186.1 (s, *C*=N), 139.8 (s, Ar*C*), 139.2 (s, Ar*C*), 138.7 (s, Ar*C*), 129.8 (s, Ar*C*), 126.2 (s, Ar*C*), 125.3 (s, Ar*C*), 115.0 (s, Mg*C*≡C), 100.3 (s, Mg*C*≡C), 45.8 (s, C*C*H$_2$C), 29.7 (s, *C*HMe$_2$), 27.9 (s, *C*HMe$_2$), 26.6 (s, NC(*C*H$_3$)), 24.7 (s, CH*C*H$_3$), 24.6 (s, CH*C*H$_3$), 23.8 (s, CH*C*H$_3$), 23.1 (s, CH*C*H$_3$), 0.2 (s, Si*Me*$_3$); ^{19}F NMR (565 MHz, $C_6H_4F_2$/benzene-d_6, 298K) δ -131.8 – -132.8 (m, 8F, *o*-C*F*), -163.6 (t, $^3J_{FF}$ = 20 Hz, 4F, *p*-C*F*), -167.4 (t, *J* = 19 Hz, 8F, *m*-C*F*); ^{11}B NMR (193 MHz, $C_6H_4F_2$/benzene-d_6, 298K) δ -16.1 (s, *B*(C$_6$F$_5$)$_4$); ^{29}Si NMR (119 MHz, $C_6H_4F_2$/benzene-d_6, 298K) δ -16.1 (s, C≡C*Si*); IR (ATR, pure): ṽ = 2970 (m), 1642 (m), 1620 (w), 1511 (s), 1461 (vs), 1372 (s), 1270 (s), 1089 (vs), 978 (vs), 841 (m), 796 (s), 754 (vs), 682 (s), 660 (s); Elemental analysis calcd (%) for $C_{116}H_{102}B_2F_{40}Mg_2N_4Si_2$ (2438.46): C 57.14, H 4.22, N 2.30; found: C 57.66, H 3.95, N 2.17.

Synthesis of {Mg$^+$C(Ph)=C(Ph)C[C(Me)=NDipp]$_2$}$_2$ 2[B(C$_6$F$_5$)$_4^-$] (4): [(BDI)Mg(*n*Pr)]$_2$ (0.085 g, 0.088 mmol) and [Ph$_3$C$^+$][B(C$_6$F$_5$)$_4^-$] (0.148 g, 0.160 mmol) were dissolved in chlorobenzene (0.5 ml) and stirred until an almost colorless solution was obtained (1 min). The solution was layered with a 0.25 M solution of diphenylacetylene in hexane (0.5 ml) and left standing at room temperature. After 1 day colorless crystals could be obtained which were washed with C_6H_5Br (2 x 0.3 ml) and hexane (4 x 0.3 ml) before they were dried in *vacuo*. The product (**4**) was isolated in a yield of 53% (0.105 g, 0.0408 mmol). One C_6H_5Cl molecule cocrystallized per dimer. Due to complete insolubility in C_6D_5Br and reversibility of the reaction in other aromatic solvents no NMR data could be acquired. IR (ATR, pure): ṽ = 2970 (m), 2934 (w), 1642 (m), 1613 (w), 1576 (m), 1512 (s), 1460 (vs), 1391 (m) 1369 (s), 1337 (m), 1297 (m), 1273 (s), 1194 (m), 1086 (vs), 977 (vs), 835 (s), 797 (s), 769 (s), 754 (s), 719 (s), 682 (s), 659

(s); Elemental analysis calcd (%) for $C_{140}H_{107}B_2ClF_{40}Mg_2N_4$ (2711.04) including one equivalent of cocrystallized C_6H_5Cl: C 62.03, H 3.98, N 2.07; found: C 62.61, H 4.06, N 1.78.

Synthesis of $\{Mg^+C(Ph)=C(Me)C[C(Me)=NDipp]_2\}_2$ $2[B(C_6F_5)_4^-]$ (5): $[(BDI)Mg(n\text{Pr})]_2$ (0.082 g, 0.085 mmol) and $[Ph_3C^+][B(C_6F_5)_4^-]$ (0.150g, 0.163 mmol) were dissolved in chlorobenzene (0.5 ml) and stirred until an almost colorless solution was obtained (1 min). The solution was layered with a 15:1 mixture of hexane/phenylpropyne (0.5 ml). After 6 d colorless crystals could be obtained which were washed with C_6H_5Br (2 x 0.3 ml) and hexane (2 x 0.3 ml) before they were dried in *vacuo*. The product was isolated in a yield of 75% (0.153 g, 0.0618 mmol). NMR data were obtained from the crystalline material (including one C_6H_5Cl molecule per dimer) in a 2:1 mixture of C_6D_5Br and C_6D_6. ^{1}H NMR (C_6D_5Br/C_6D_6, 600 MHz, 298K) δ 7.38 (t, $^3J_{HH}$ = 7.6 Hz, 2H,C=C*Ph*), 7.25 (t, $^3J_{HH}$ = 7.7 Hz, 2H, Dipp–Ar*H*), 7.17 – 7.11 (m, 4H, Ar*H*), 6.97 – 6.94 (m, 1H, C=C*Ph*), 6.62 (d, $^3J_{HH}$ = 7.3 Hz, 2H, C=C*Ph*), 4.39 (s, 1H, CC*H*$(CN)_2$), 2.48 (hept, $^3J_{HH}$ = 6.8 Hz, 2H, C*H*Me_2), 2.28 (hept, $^3J_{HH}$ = 6.8 Hz, 2H, C*H*Me_2), 1.74 (s, 3H, C=CC*H*$_3$), 1.61 (s, 6H, NCC*H*$_3$), 1.29 (d, $^3J_{HH}$ = 6.8 Hz, 6H, CHC*H*$_3$), 1.11 (d, $^3J_{HH}$ = 6.8 Hz, 6H, CHC*H*$_3$), 0.90 (d, $^3J_{HH}$ = 6.8 Hz, 6H, CHC*H*$_3$), 0.83 (d, $^3J_{HH}$ = 6.8 Hz, 6H, CHC*H*$_3$); ^{13}C NMR (C_6D_5Br/C_6D_6, 151 MHz, 298K) δ 182.5 (s, *C*=N), 175.1 (s, C=*C*Ph), 149.0 (d, $^1J_{CF}$ = 241 Hz, B(C_6F_5)$_4$), 147.7 (s, C=C*Ph*), 140.0 (s, Dipp-Ar*C*) 139.46 (s, C=C*Ph*), 138.66 (s, Dipp-Ar*C*), 136.91 (d, $^1J_{CF}$ = 255 Hz, B(C_6F_5)$_4$), 132.4 (s, C=*C*CH_3), 129.9 (s, C=C*Ph*), 128.8 (s, C=C*Ph*), 128.7 (s, Dipp-Ar*C*), 125.4 (s, C=C*Ph*), 125.0 (s, Dipp-Ar*C*), 64.5 (s, C*C*H$(CN)_2$), 29.3 (s, *C*HMe_2), 28.1 (s, *C*H$(CH_3)_2$), 27.4 (s, NC*C*H$_3$), 24.4 (s, CH(*C*H$_3$)$_2$), 24.2 (s, CH(*C*H$_3$)$_2$), 24.1 (s, CH(*C*H$_3$)$_2$), 23.9 (s, CH(*C*H$_3$)$_2$), 22.1 (s, C=C*C*H$_3$); ^{19}F NMR (C_6D_5Br/C_6D_6, 565 MHz, 298K) δ -130.5 – -132.5 (m, 8F, *o*-C*F*), -161.9 (t, $^3J_{FF}$ = 21 Hz, 4F, *p*-C*F*), -165.8 (t, *J* = 20 Hz, 8F, *m*-C*F*); ^{11}B NMR (C_6D_5Br/C_6D_6, 193 MHz, 298K) δ -15.8 (s, *B*(C_6F_5)$_4$); IR (ATR, pure): ṽ = 2968 (m), 2932 (w), 2875 (w), 1642 (m), 1614 (w), 1583 (w), 1512 (s), 1460 (vs), 1369 (s), 1273 (s), 1187 (w), 1087 (vs), 976 (vs), 843 (m), 797 (s), 772 (s), 756 (s), 747 (s), 682 (s), 660 (s); Elemental analysis calcd (%) for $C_{124}H_{98}B_2F_{40}Mg_2N_4$ (2474.34): C 60.19, H 3.99, N 2.26; found: C 59.64, H 4.03, N 1.89.

***In situ* generation of $[(BDI)Mg^+{\cdot}PPh_3][B(C_6F_5)_4^-]$ (6):** *In situ* generation of $[(BDI)Mg^+{\cdot}PPh_3][B(C_6F_5)_4^-]$ was accomplished by dissolving $[(BDI)Mg^+{\cdot}C_6H_6][B(C_6F_5)_4^-]$ (0.0140 g, 0,0117 mmol) and PPh_3 (0.0031 g, 0.012 mmol) in C_6D_5Br (0.5 ml). For crystallization of the product, $[(BDI)Mg^+{\cdot}C_6H_6][B(C_6F_5)_4^-]$ (0.0412g, 0.0344 mmol) and substoichiometric quantities of PPh_3 (0.0042 g, 0.016 mmol) were dissolved in a 2:1 mixture of chlorobenzene (0.4 ml)

and toluene (0.2 ml) and the resulting solution was layered with hexane (0.5 ml). A few colorless crystals suitable for X–ray diffraction could be isolated after 30 days. NMR data are given for the *in situ* generated adduct. ^{1}H NMR (C_6D_5Br, 400 MHz, 298 K) δ 7.26 – 7.16 (m, 5H, Ar*H*), 7.04 (d, $^{3}J_{HH}$ = 7.7 Hz, 4H, Dipp–Ar*H*), 7.03 – 6.95 (m, 6H, P*Ph*$_3$), 6.52 (dd, $^{3}J_{PH}$ = 12.3 Hz, $^{3}J_{HH}$ = 7.7 Hz, 6H, PCC*H*C) 4.97 (s, 1H, CC*H*C), 2.84 (hept, *J* = 6.8 Hz, 4H, C*H*(CH$_3$)$_2$), 1.57 (s, 6H, NCC*H*$_3$), 1.01 (d, $^{3}J_{HH}$ = 6.8 Hz, 12H, CH(C*H*$_3$)$_2$), 0.63 (d, $^{3}J_{HH}$ = 6.8 Hz, 12H, CH(C*H*$_3$)$_2$; ^{13}C NMR (C_6D_5Br, 101 MHz, 298 K) δ 173.2 (s, *C*CH*C*), 149.1 (d, $^{1}J_{CF}$ = 233 Hz, B(C_6F_5)$_4$), 143.0 (s, Ar*C*), 142.4 (s, Ar*C*), 138.9 (d, $^{1}J_{CF}$ = 240 Hz, B(C_6F_5)$_4$), 137.1 (d, $^{1}J_{CF}$ = 242 Hz, B(C_6F_5)$_4$), 133.1 (d, $^{2}J_{CP}$ = 14 Hz, P*Ph*$_3$), 132.6 (d, $^{4}J_{CP}$ = 3 Hz, P*Ph*$_3$), 130.6 (d, $^{3}J_{CP}$ = 11 Hz, P*Ph*$_3$) 127.6 (s, Ar*C*), 125.3 (s, Ar*C*), 97.8 (s, C*C*HC), 29.1 (s, *C*H(CH$_3$)$_2$), 24.8 (s, CH(*C*H$_3$)$_2$), 24.7 (s, NCC*H*$_3$), 24.1 (s, CH(*C*H$_3$)$_2$), (the quaternary carbon in PPh_3 is not observed); ^{31}P{^{1}H} NMR (C_6D_5Br, 162 MHz, 298 K) δ -5.0 (s, *P*Ph$_3$); ^{19}F NMR (C_6D_5Br, 376 MHz, 298 K): δ -129.8 – -132.0 (m, 8F, *m*-Ar*F*), −161.4 (t, $^{3}J_{FF}$ = 21 Hz, 4F, *p*-Ar*F*), −165.6 (t, $^{3}J_{FF}$ = 20 Hz, 8F, *o*-Ar*F*) ppm; ^{11}B NMR (C_6D_5Br, 128 MHz, 298 K): δ −15.6 (s, *B*(C_6F_5)$_4$) ppm.

Synthesis of [(BDI)Mg^{+}·PCy$_3$][B(C_6F_5)$_4^{-}$] (7): *In situ* generation of [(BDI)Mg^{+}·PCy$_3$][B(C_6F_5)$_4^{-}$] was accomplished by dissolving [(BDI)Mg^{+}·C_6H_6][B(C_6F_5)$_4^{-}$] (0.0141 g, 0,0118 mmol) and PCy$_3$ (0.0033 g, 0.0118 mmol) in C_6D_5Br (0.5 ml). For crystallization of the product, [(BDI)Mg^{+}·C_6H_6][B(C_6F_5)$_4^{-}$] (0.1489 g, 0.1242 mmol) and PCy$_3$ (0.0427 g, 0.152 mmol) were dissolved in fluorobenzene (1.0 ml) and the resulting solution was layered with hexane (1.0 ml). Colorless crystals could be isolated after 3 days in a yield of 5% (0.010 g, 0.0068 mmol). The complex crystallized with one PhF molecule. ^{1}H NMR (C_6D_5Br, 400 MHz, 298 K) δ 7.13 – 7.00 (m, 6H, Ar*H*), 5.00 (s, 1H, CC*H*C), 2.83 (hept, $^{3}J_{HH}$ = 6.8 Hz, 4H, C*H*(CH$_3$)$_2$), 1.56 (s, 6H, NCC*H*$_3$), 1.62 – 1.39 (m, 12H, P*Cy*$_3$), 1.12 (d, $^{3}J_{HH}$ = 6.8 Hz, 12H, CH(C*H*$_3$)$_2$), 1.09 (d, $^{3}J_{HH}$ = 6.8 Hz, 12H, CH(C*H*$_3$)$_2$), 1.18 – 1.05 (m, 3H, PC*H*CH$_2$), 1.00 – 0.76 (m, 12H, P*Cy*$_3$), 0.75 – 0.57 (m, 6H, P*Cy*$_3$); ^{13}C NMR (C_6D_5Br, 101 MHz, 298 K) δ 173.3 (s, *C*CH*C*), 149.1 (d, $^{1}J_{CF}$ = 241 Hz, B(C_6F_5)$_4$), 142.9 (s, Ar*C*), 142.0 (s, Ar*C*), 138.8 (d, $^{1}J_{CF}$ = 244 Hz, B(C_6F_5)$_4$), 137.0 (d, $^{1}J_{CF}$ = 247 Hz, B(C_6F_5)$_4$), 127.9 (s, Ar*C*), 125.1 (s, Ar*C*), 98.1 (s, C*C*HC), 31.1 (s, P*Cy*$_3$) , 30.8 (d, $^{2}J_{CP}$ = 16 Hz, P*C*H), 29.4 (s, *C*H(CH$_3$)$_2$), 27.3 (d, $^{3}J_{CP}$ = 11 Hz, *o*–Cy), 25.4 (s, P*Cy*$_3$), 25.3 (s, CH(*C*H$_3$)$_2$), 25.0 (s, NCC*H*$_3$), 24.2 (s, CH(*C*H$_3$)$_2$); ^{31}P{^{1}H} NMR (C_6D_5Br, 162 MHz, 298 K) δ 20.4 (s, *P*Cy$_3$); ^{19}F NMR (C_6D_5Br, 376 MHz, 298 K): δ -130.0 – -132.5 (m, 8F, *m*-Ar*F*), −161.8 (t, $^{3}J_{FF}$ = 19 Hz, 4F, *p*-Ar*F*), −165.2 – -165.7 (m, 8F, *o*-Ar*F*) ppm; ^{11}B NMR (C_6D_5Br, 128 MHz, 298 K): δ

−15.6 (s, $B(C_6F_5)_4$) ppm. Elemental analysis calcd (%) for $C_{77}H_{79}BF_{20}MgN_2P$ (1497.55): C 61.76%, H 5.32%, N 1.87%. Found: 61.83%, H 5.08%, N 1.96%.

***In situ* generation of [(BDI)Mg⁺·P*t*Bu₃][B(C₆F₅)₄⁻] (8):** *In situ* generation of [(BDI)Mg⁺·P*t*Bu₃][B(C₆F₅)₄⁻] was accomplished by dissolving [(BDI)Mg⁺·C₆H₆][B(C₆F₅)₄⁻] (0.0092 g, 0,0077 mmol) and P*t*Bu₃ (0.0016 g, 0.0080 mmol) in a 2:1 mixture of C_6H_5Cl/C_6D_6 (0.5 ml). NMR analysis showed that the phosphine adduct (**8**) is in equilibrium with the benzene adduct (BDI)Mg⁺·C₆H₆. For crystallization of the product, [(BDI)Mg⁺·C₆H₆][B(C₆F₅)₄⁻] (0.0505 g, 0.0421 mmol) and P*t*Bu₃ (0.0085 g, 0.0420 mmol) were dissolved in a 2:1 mixture of benzene (0.4 ml) and fluorobenzene (0.2 ml). The solution was allowed to evaporate to dryness at room temperature. From the residue it was possible to obtain a few colorless crystals suitable for X-ray diffraction that were embedded in amorphous material. NMR data are given for the *in situ* generated adduct. From the two species that are in equilibrium only data for [(BDI)Mg⁺·P*t*Bu₃][B(C₆F₅)₄⁻] are given. ^{1}H NMR (C_6D_6/C_6H_5Cl, 600 MHz, 298 K) δ 4.98 (s, 1H, CC*H*C), 2.71 (hept, $^3J_{HH}$ = 6.7 Hz, 4H, C*H*$(CH_3)_2$), 1.55 (s, 6H, NCC*H*$_3$), 1.07 (d, $^3J_{HH}$ = 6.7 Hz, 12H, CH(C*H*$_3)_2$), 0.99 (d, $^3J_{HH}$ = 6.7 Hz, 12H, CH(C*H*$_3)_2$), 0.68 (d, $^3J_{PH}$ = 13.8 Hz, 27H, P^t*Bu*$_3$). (all signals in the aromatic region are obscured by $C_6H_4F_2$); ^{13}C NMR (C_6D_6/C_6H_5Cl, 151 MHz, 298 K) δ 172.9 (s, *C*CH*C*), 148.7 (d, $^1J_{CF}$ = 243 Hz, $B(C_6F_5)_4$), 143.6 (s, Ar*C*), 141.5 (s, Ar*C*), 138.4 (d, $^1J_{CF}$ = 244 Hz, $B(C_6F_5)_4$), 136.6 (d, $^1J_{CF}$ = 247 Hz, $B(C_6F_5)_4$), 128.2 (s, Ar*C*), 124.8 (s, Ar*C*), 97.2 (s, C*C*HC), 35.7 (d, $^1J_{CP}$ = 5.8 Hz, P*C*$(CH_3)_3$) , 31.4 (d, $^2J_{CP}$ = 5.2 Hz, PC(*C*H$_3)_3$), 29.3 (s, *C*H$(CH_3)_2$), 25.3 (s, NCC*H*$_3$), 24.1 (s, CH(*C*H$_3)_2$), 23.6 (s, CH(*C*H$_3)_2$); ^{31}P{^{1}H} NMR (C_6D_6/C_6H_5Cl, 243 MHz, 298 K) δ 69.7 (s, *P*^{t}Bu$_3$); ^{19}F NMR (C_6D_6/C_6H_5Cl, 565 MHz, 298 K): δ -130.5 – -132.5 (m, 8F, *m*-Ar*F*), −162.4 (t, $^3J_{FF}$ = 20 Hz, 4F, *p*-Ar*F*), −166.5 (t, $^3J_{FF}$ = 20 Hz, 8F, *o*-Ar*F*) ppm; ^{11}B NMR (C_6D_5Br, 193 MHz, 298 K): δ −16.1 (s, $B(C_6F_5)_4$) ppm.

Supporting Information

Additional data for complex [(BDI)Mg⁺·EtCCEt][B(C₆F₅)₄⁻] (IR, Raman), NMR spectra for complexes **2–3** and **5**–**8**, IR spectra for complexes **2**–**5** and details for the crystal structure determinations of complexes **2**-**8**.

Author Information

Corresponding author: sjoerd.harder@fau.de

The authors declare no competing financial interest.

Acknowledgements

We acknowledge Mrs. C. Wronna (University of Erlangen-Nürnberg) for numerous CHN analyses and J. Schmidt and Dr. C. Färber (University of Erlangen-Nürnberg) for assistance with the NMR analyses. We acknowledge Boulder Scientific for a sample of $[Ph_3C^+][B(C_6F_5)_4^-]$.

References:

[1] a) A. Corma, H. García, *Chem. Rev.* **2003**, *103*, 4307–4366. b) J. R. Lawson, R. L. Melen, *Inorg. Chem.* **2017**, *56*, 8627–8643. c) J. M. Bayne, D. W. Stephan, *Chem. Soc. Rev.* **2016**, *45*, 765–774.

[2] B. Liu, V. Dorcet, L. Maron, J. F. Carpentier, Y. Sarazin, *Eur. J. Inorg. Chem.* **2012**, 3023–3031.

[3] J. Pahl, S. Brand, H. Elsen, S. Harder, *Chem. Commun.* **2018**, *54*, 8685–8688.

[4] J. Pahl, H. Elsen, A. Friedrich, S. Harder, *Chem. Commun.* **2018**, *54*, 7846–7849.

[5] S. Harder, S. Brand, H. Elsen, J. Langer, W. A. Donaubauer, F. Hampel, *Angew. Chemie Int. Ed.* **2018**, *0*, DOI 10.1002/anie.201809236.

[6] a) S. Brand, J. Pahl, H. Elsen, S. Harder, *Eur. J. Inorg. Chem.* **2017**, *2017*, 4187–4195. b) J. Langer, I. Kosygin, R. Puchta, J. Pahl, S. Harder, *Chem. - Eur. J.* **2016**, *22*, 17425–17435.

[7] H. V. Rasika Dias, J. A. Flores, J. Wu, P. Kroll, *J. Am. Chem. Soc.* **2009**, *131*, 11249–11255.

[8] Y. Yu, J. M. Smith, C. J. Flaschenriem, P. L. Holland, *Inorg. Chem.* **2006**, *45*, 5742–51.

[9] F. H. Allen, O. Kennard, D. G. Watson, L. Brammer, A. G. Orpen, R. Taylor, *J. Chem. Soc. Perkin Trans. 2* **1987**, *213*, S1.

[10] a) G. A. Crowder, P. Blankenship, *J. Mol. Struct.* **1987**, *156*, 147–150. b) H.-H. Perkampus, W. Weiss, Z. Naturforsch. **1974**, *29b*, 61–64.

[11] J. Pahl, A. Friedrich, H. Elsen, S. Harder, *Organometallics* **2018**, acs.organomet.8b00489.

[12] O. J. Metters, S. J. K. Forrest, H. A. Sparkes, I. Manners, D. F. Wass, *J. Am. Chem. Soc.* **2016**, *138*, 1994–2003.

[13] M. Arrowsmith, M. R. Crimmin, M. S. Hill, S. L. Lomas, D. J. MacDougall, M. F. Mahon, *Organometallics* **2013**, *32*, 4961–4972.

[14] F. G. Bordwell, G. E. Drucker, N. H. Andersen, A. D. Denniston, *J. Am. Chem. Soc.* **1986**, *108*, 7310–7313.

[15] C. Camp, J. Arnold, *Dalton Trans.* **2016**, *45*, 14462–14498.

[16] A. Friedrich, J. Pahl, H. Elsen, S. Harder, *Dalton Trans* **2018**, *submitted manuscript.*

[17] a) H. Lehmkuhl, K. Mehler, R. Benn, A. Rufinska, C. Krüger, *Chem. Ber.* **1986**, *119*, 1054–1069. b) D. E. Gindelberger, J. Arnold, *Inorg. Chem.* **1994**, *33*, 6293–6299. c) L. Garcia, M. D. Anker, M. F. Mahon, L. Maron, M. S. Hill, *Dalton Trans.* **2018**, DOI 10.1039/C8DT03124J.

[18] T. E. Müller, D. M. P. Mingos, *Transition Met. Chem.* **1995**, *20*, 533–539.
[19] T. E. Stennett, J. Pahl, H. S. Zijlstra, F. W. Seidel, S. Harder, *Organometallics* **2016**, *35*, 207–217.
[20] Y. Moglie, M. J. González-Soria, I. Martín-García, G. Radivoy, F. Alonso, *Green Chem.* **2016**, *18*, 4896–4907.
[21] L. Keweloh, H. Klöcker, E.-U. Würthwein, W. Uhl, *Angew. Chemie Int. Ed.* **2016**, *55*, 3212-3215.
[22] M. Reißmann, A. Schäfer, S. Jung, T. Müller, *Organometallics* **2013**, *32*, 6736–6744.